Pygmy dipole resonance built on the shape-isomeric state in ^{68}Ni

Xuwei Sun, Jing Chen, and Dinghui Lu
Department of Physics, Zhejiang University, 310027 Hangzhou, China

(Received 30 May 2018; published 9 August 2018)

The pygmy dipole resonance (PDR) of ^{68}Ni was measured by Wieland *et al.* [Phys. Rev. Lett. **102**, 092502 (2009)] through virtual photon scattering and Rossi *et al.* [Phys. Rev. Lett. **111**, 242503 (2013)] through a photoneutron reaction. However, the PDR peaks are observed at different positions: 11 and 9.55(17) MeV respectively. Our calculation based on the deformed relativistic random phase approximation suggests that the discrepancy between these two measurements might be induced by the effect of the shape-coexistence isomeric state in ^{68}Ni.

DOI: 10.1103/PhysRevC.98.024607

I. INTRODUCTION

The low-lying responses of a nucleus to an external electric field can provide abundant information about nuclear structure and excitation properties. Among them, the pygmy dipole resonance (PDR) has been intensely discussed in recent years, and fruitful achievements have been realized [1–6]. The PDR is closely related to the neutron skin thickness [7–10] and is expected to introduce meaningful constraints on the parameters important to the nuclear equation of state, such as the slope of symmetry energy L [11]. In the light nucleus ^{11}Li, the picture of this soft mode was proposed by Jonson [12] and Suzuki [13] as the relative motion between two valence neutrons and a ^{9}Li core. With enormous efforts for years, it has been shown that this low-lying excitation mode, typically emerging in neutron-rich nuclei, is induced by the loosely bound valence neutrons oscillating against a compact isospin-saturated core. It has been reported in some nuclei, such as ^{138}Ba, ^{140}Ce [14], and ^{124}Sn [15], that the low-lying electric dipole strength splits into two different types. One of them, having isovector character, can be observed in both $(\alpha, \alpha'\gamma)$ and (γ, γ') reactions, while the other can be observed only in $(\alpha, \alpha'\gamma)$ experiments and has isoscalar character. Whether the isovector part of the pygmy dipole excitation is the low energy tail of the giant dipole resonance (GDR) is still an open question. Therefore, in this work, we regard the main part of PDR as isoscalar vibrations.

The PDR of the unstable neutron-rich nucleus ^{68}Ni has been measured in recent years. However, there is a strong discrepancy between the results deduced from virtual photon scattering (γ^*, γ) [9] and photoneutron (γ^*, n), $(\gamma^*, 2n)$ reactions [16], where γ^* represents a virtual photon. In both measurements mentioned above, the beams of ^{68}Ni are produced by bombarding a Be target using ^{86}Kr. In the former case, i.e., (γ^*, γ), the electromagnetic excitations of ^{68}Ni ions are achieved by impinging them on an Au target and the γ rays emitted at the target location are measured. In the latter case, the electromagnetic excitation is introduced by using a Pb target and the invariant mass in one- and two-neutron decay channels is measured. The low-lying photoabsorption spectra have been constructed and the PDR peaks are observed at 11 and 9.55(17) MeV respectively. Details of the experimental setups can be found in the related references [16,17]. The shift of the PDR peak positions has been discussed by the authors of Ref. [16] due to a possibly energy-dependent branching ratio. However, our study shows this might be explained as the PDR being built on different shape states, i.e., the spherical ground state and the shape isomeric state with prolate geometry.

The appearance of isomeric states is an interesting phenomenon in atom nuclei. In theoretical research, usually the primary minimum of the potential-energy surface (PES) is interpreted as the ground state of a nucleus, and in some nuclei there is a secondary minimum (or several minima, separated by energy barriers) which implies the occurrence of a metastable state, such as a spin isomer, K isomer, shape isomer [19], etc. Shape coexistence is thought to be important to interpret the observed irregular yrast sequence in some nuclei [20], and the relationship between shape coexistence and phase transition is currently under debate [21,22]. The shape coexistence has been found in many spherical nuclei near magic shells, e.g., the nucleus ^{68}Ni has been studied for years and several isomeric states, both prolate and oblate, have been identified [23,24]. The first isomeric state (0_2^+) was reported lying at 1604 keV [25] with a lifetime of about $\tau = 390$ ns [26]. Such an isomeric state is implied in some relativistic mean field models, like DD-ME2 [27] and NL3 [28], as a secondary local minimum in the PES at $(\beta \approx 0.4, \gamma = 0^\circ)$, where β and γ are Hill-Wheeler coordinates [29], as demonstrated in Fig. 1.

The ^{68}Ni nucleus has a magic proton number 28 and the neutrons fill up to pf orbitals, which makes the ground state of this semiclosed nucleus spherical. In contrast, the prolate geometry has a different particle-hole content: there is a severe shell mixing between pf and $1g_{9/2}$ orbitals. The shape isomeric state acquires extra freedom through the breaking of the rotation symmetry; it will definitely respond to external electromagnetic perturbations in a different way when compared to its spherical partner. This might be the missing part to solve the conflict between different PDR measurements in ^{68}Ni.

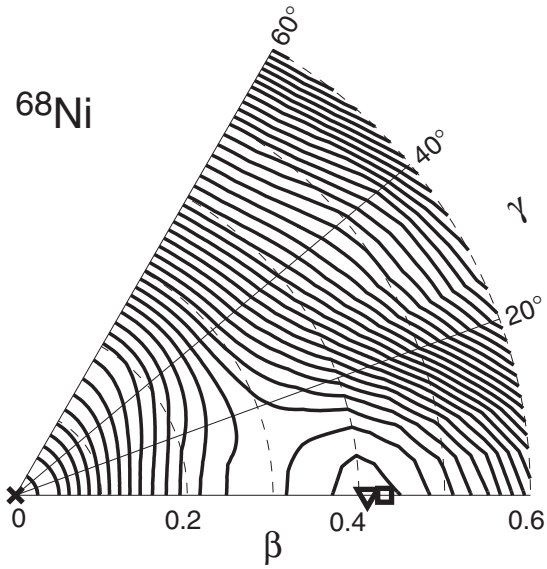

FIG. 1. PES of ^{68}Ni predicted by the relativistic nuclear force DD-ME2, generated using the code in [18]. Apart from the spherical ground state (marked by $\times$), there is a prolate shape isomer (marked by $\triangledown$) at ($\beta \approx 0.4$, $\gamma = 0^\circ$). The NL3 model predicts a similar secondary minimal and is marked by $\square$. The contours are drawn with spacings of 0.5 MeV.

II. METHOD AND RESULT

Concerning the small amplitude vibrations in the vicinity of an equilibrium position, the random phase approximation (RPA) method [30] is a useful tool that is widely used in the research of low-lying nuclear excitations in closed shell nuclei [31,32]. The generalization of the RPA method by including pairing correlations, namely, the quasiparticle random phase approximation (QRPA) method, also has been developed in a self-consistent framework [33] and has been applied in the study of charge-exchange excitations [34,35]. Under the nonspherical symmetry condition, the dimension of the QRPA matrix increases rapidly and the diagonalization of the QRPA equation becomes a serious numerical challenge. By truncating the configuration space, some nonspherical QRPA calculations have been performed [36,37]. Otherwise, the finite amplitude method (FAM) is an alternative approach if one does not need the details of every excited state [38,39]. Meanwhile, we notice that the effect of the pairing correlation on PDR is relatively small [40,41], and is sometimes omitted in related studies [42,43]. Therefore, in this work, we adopt a deformed relativistic RPA approach, assuming that the effect of the pairing interaction on the results is mild and focusing on the deformed isomeric state. Our RPA calculation is implemented in a relativistic framework and is fully self-consistent; the interaction used in the determination of the nuclear stationary state and the evaluation of excitation properties are the same. Moreover, the influence of the antiparticle states and the time-odd components of meson fields are both considered.

The energy of the nuclear system can be described by a functional of the density operator $\hat{\rho}$ [30],

$$E[\rho] = \mathrm{Tr}(\epsilon\rho) + \tfrac{1}{2}\mathrm{Tr}\,\mathrm{Tr}(\rho V \rho), \tag{1}$$

where ϵ is the kinetic energy and the single-particle Hamiltonian is defined by $\hat{h} = \delta E/\delta\hat{\rho}$. In the single-particle space, the static parts of the density operator and the single-particle Hamiltonian are simple, i.e., $\rho^0_{kl} = \rho_k\delta_{kl}$ and $h^0_{kl} = \epsilon_k\delta_{kl}$, where $\rho_k = 1$ for "hole" states (below Fermi level) and $\rho_k = 0$ for "particle" states (above Fermi level, also including the antiparticle states in the Dirac sea). Under the small amplitude approximation,

$$\rho(t) = \rho^0 + \delta\rho(\omega)e^{-i\omega t} + \delta\rho^\dagger(\omega)e^{i\omega t}. \tag{2}$$

$\hat{\rho}$ is a projector operator; that means $\hat{\rho}^2 = \hat{\rho}$. Therefore, the nonvanishing matrix elements of the transition density are $\delta\rho_{ph}$ and $\delta\rho_{hp}$, which leads to the variation of the single-particle Hamiltonian,

$$\delta h = \frac{\partial h}{\partial\rho}\delta\rho = \sum_{ph}\frac{\partial h}{\partial\rho_{ph}}\delta\rho_{ph} + \sum_{hp}\frac{\partial h}{\partial\rho_{hp}}\delta\rho_{hp}. \tag{3}$$

Substituting the above equations into the equation of motion of the density operator, i.e.,

$$i\,\partial_t\hat{\rho} = [\hat{h}, \hat{\rho}], \tag{4}$$

then leaves us coupled equations for $\delta\rho_{ph}$ and $\delta\rho_{hp}$, which can be expressed as

$$\begin{pmatrix} A & B \\ B^* & A^* \end{pmatrix}\begin{pmatrix} X \\ Y \end{pmatrix} = \omega\begin{pmatrix} 1 & 0 \\ 0 & -1 \end{pmatrix}\begin{pmatrix} X \\ Y \end{pmatrix} \tag{5}$$

by introducing

$$\begin{aligned} A_{php'h'} &\equiv (\epsilon_p - \epsilon_h)\delta_{pp'}\delta_{hh'} + V_{ph'hp'}, \\ B_{php'h'} &\equiv V_{pp'hh'}. \end{aligned} \tag{6}$$

Here X and Y denote $\delta\rho_{ph}$ and $\delta\rho_{hp}$ respectively, and the matrix elements of the residual interaction are defined by

$$V_{abcd} \equiv \frac{\partial h_{ac}}{\partial\rho_{db}}. \tag{7}$$

In our study, the relativistic mean filed force NL3 [28] is used, the nucleons interact with each other via exchanging σ, $\boldsymbol{\omega}$, $\vec{\boldsymbol{\rho}}$ mesons and photon γ. The two-body interaction reads

$$\begin{aligned} V(\boldsymbol{r}_1, \boldsymbol{r}_2) = &- g_\sigma\beta^1 G_\sigma(\boldsymbol{r}_1, \boldsymbol{r}_2) g_\sigma\beta^2 \\ &+ g_\omega\beta^1\gamma^\mu G_\omega(\boldsymbol{r}_1 - \boldsymbol{r}_2) g_\omega\beta^2\gamma_\mu \\ &+ g_\rho\tau_3^1\beta^1\gamma^\mu G_\rho(\boldsymbol{r}_1 - \boldsymbol{r}_2) g_\rho\tau_3^2\beta^2\gamma_\mu \\ &+ e^2\frac{1-\tau_3^1}{2}G_\gamma(\boldsymbol{r}_1 - \boldsymbol{r}_2)\frac{1-\tau_3^2}{2}, \end{aligned} \tag{8}$$

where $g_{\sigma,\omega,\rho}$ is the coupling constants. The propagators of $\boldsymbol{\omega}$, $\vec{\boldsymbol{\rho}}$, γ have Yukawa form $e^{-m|\boldsymbol{r}_1-\boldsymbol{r}_2|}/4\pi|\boldsymbol{r}_1 - \boldsymbol{r}_2|$, while, for the σ meson, the form depends on the self-coupling $U(\sigma)$, which is essential for a reasonable description of the nuclear incompressibility [44] and can be solved from the Klein-Gordon equation

$$\left[-\Delta + m_\sigma^2 + U''(\sigma)\right]G_\sigma(\boldsymbol{r}_1, \boldsymbol{r}_2) = -\delta(\boldsymbol{r}_1 - \boldsymbol{r}_2). \tag{9}$$

The matrix elements of the residual interaction are calculated by expanding the single-particle wave functions using a deformed harmonic oscillator basis [45]. The calculation details as well as the validation of the numerical implementation,

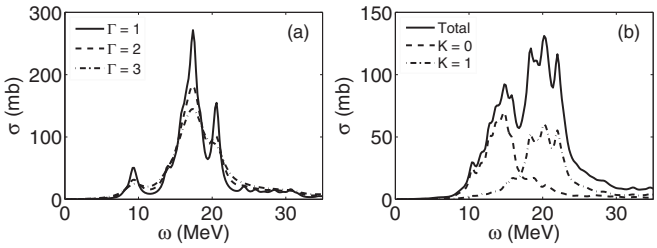

FIG. 2. (a) Cross section obtained in the spherical case, smeared with different width Γ (in MeV). (b) The solid line (Total) denotes the cross section built on the prolate isomeric state, and the dashed (dash-dotted) line denotes the $K = 0$ ($K = 1$) part.

especially the decoupling of the spurious states, can be found in our previous work [46].

Diagonalizing the RPA equation (5) in the vicinity of the spherical (SPH.) ground state and the prolate (PRO.) isomeric state respectively, we will get two sets of transition densities, $\{X_{ph}^{\nu,\mathrm{SPH.}}, Y_{ph}^{\nu,\mathrm{SPH.}}\}$ and $\{X_{ph}^{\nu,\mathrm{PRO.}}, Y_{ph}^{\nu,\mathrm{PRO.}}\}$, as well as the excited energies $\omega_\nu^{\mathrm{SPH.}}$ and $\omega_\nu^{\mathrm{PRO.}}$. The transition densities X and Y are used to calculate the transition matrix elements of the electric dipole operator through

$$\langle 0|\hat{E}1|\nu\rangle = \sum_{ph} \hat{E}1_{hp} X_{ph}^{\nu} + \hat{E}1_{ph} Y_{ph}^{\nu}, \tag{10}$$

where $|0\rangle$ is either the spherical ground state $|\mathrm{SPH.}\rangle$ or the prolate isomeric state $|\mathrm{PRO.}\rangle$, and $|\nu\rangle$ denotes the excited state built on them correspondingly, i.e., $|\nu, \mathrm{SPH.}\rangle$ or $|\nu, \mathrm{PRO.}\rangle$. The electric dipole operator can be expressed with the recoil charge as [47]

$$\hat{E}_{1\mu} = \frac{Ne}{N+Z} \sum_{p=1}^{Z} r_p Y_{1\mu} - \frac{Ze}{N+Z} \sum_{n=1}^{N} r_n Y_{1\mu}. \tag{11}$$

In order to get a continuous strength function, a Lorentzian function is used to smear the discrete transition probabilities relating to RPA states [48],

$$R(\omega) = \sum_{\nu} |\langle \nu||\hat{E}1||0\rangle|^2 \frac{1}{\pi} \frac{\Gamma/2}{(\omega-\omega_\nu)^2 + (\Gamma/2)^2}, \tag{12}$$

and the photoabsorption cross section reads [8]

$$\sigma(\omega) = \frac{16\pi^3 e^2}{9\hbar c} \omega R(\omega). \tag{13}$$

Γ is the width of the Lorentzian distribution; it controls the sharpness of the distribution while having no effects on the peak position. In Fig. 2(a), the cross section built on the spherical ground state is smeared with different widths; the larger Γ is, the more the peak is flattened.

The cross sections in these two cases have distinct behavior both in the pygmy energy region (0–12 MeV) and the giant energy region (12–35 MeV). In the giant energy region, the dipole transition strength in the prolate case splits into two wide peaks, mainly because the shape isomeric state is axially deformed. From Fig. 2(b) we learn that the peak originating from the $K^\pi = 1^-$ channel is located higher than the peak in the $K^\pi = 0^-$ channel. In the spherical case, the $K = 0$ part and the

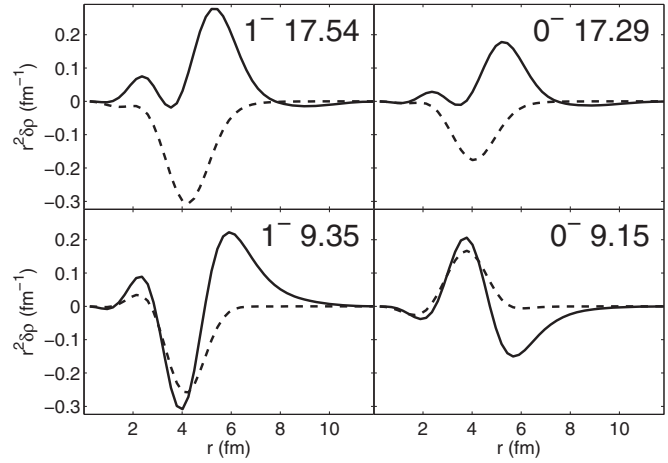

FIG. 3. The radial distribution of the dominant states contributing to PDR and GDR in nucleus ^{68}Ni, excited from the spherical ground state. The density belonging to neutrons (protons) is expressed with a solid (dash) line. The quantum number (K^π) and energy (in MeV) of each state is labeled at the up right corner.

$K = 1$ part coincide. In the pygmy resonance region, the PDR peak is well separated in the spherical case; however, in the prolate case, GDR and PDR overlap significantly. Therefore, it is necessary to separate the resonance structure belonging to PDR in order to evaluate the related cross section correctly. Such a requirement can be fulfilled by picking out the excited states with strong isoscalar character, which will be revealed in detail in the following context.

The radial distribution of the transition density $\delta\hat{\rho}$ in the axial symmetry case can be projected from the intrinsic frame to the laboratory frame through

$$\delta\rho_L(r) = \int d\cos\theta\, d\varphi\, \delta\rho(r_\perp, z) Y_{1K}^*(\theta,\varphi). \tag{14}$$

The isospin property of an excited state can be determined by the transition density's radial distribution, i.e., according to whether neutrons and protons oscillate in phase or out of phase. For instance, the GDR levels are induced by the relative motion of neutrons against protons, therefore they have strong isovector characters. In the PDR area, the dominant excited states are caused by the vibration of excess neutrons, and the neutrons and protons are oscillating in phase. The typical types of the transition densities corresponding to GDR and PDR built on the spherical ground state are shown in Fig. 3. It is easy to see that in most areas the transition densities of neutrons and protons have opposite signs (out of phase) for GDR levels, while for PDR the situation reverses. In a quantitative analysis, for example, one can label a state as "isoscalar" if the radial distribution of neutrons and protons oscillate in phase in more than 70% of the area. Such a treatment was proposed by Paar *et al.* [5] (called "IS" percentage). Here, based on the distinct patterns of the radial distribution, we define a coefficient

$$R = \frac{\int r^2 |\delta\rho_p(r) + \delta\rho_n(r)|^2 dr}{\int r^2 |\delta\rho_p(r) - \delta\rho_n(r)|^2 dr}, \tag{15}$$

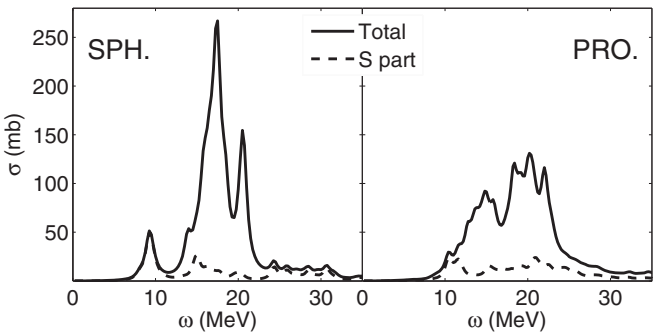

FIG. 4. Electric dipole excitations built on the spherical ground state (SPH.) and the prolate isomeric state (PRO.) in ^{68}Ni. The total photoabsorption cross section and the isospin-scalar part are illustrated with solid lines (Total) and dashed lines (S part), respectively. The smear width used in the calculation is $\Gamma = 1$ MeV.

to describe the isospin character of an excited state. The isoscalar states have rather large R's while isovector states have relatively small ones. (For states with strong isoscalar and isovector characters, R's differ by one order of magnitude. For convenience, $R = 1$ is chosen in our work as the criterion to distinguish isoscalar states and isovector ones.)

The isoscalar part of the electric dipole resonance can be separated by picking out RPA excited states with $R > 1$, and the corresponding cross section are generated, as the "S part" illustrated in Fig. 4 with dashed lines. In the spherical case, almost the whole low-lying cross section is exhausted by PDR, while in the prolate case the low-lying part contains some mixing from GDR tails and can be ruled out by R. Once the pygmy resonance is separated, it is clear that the peak in prolate case (right panel) shifts to higher energy. The centroid energiy $E_{\rm cen} = m_1/m_0$ is 10.89 MeV, where ith energy weighted moment m_i [30] is evaluated in the energy region 8–13 MeV. In the spherical case (left panel), the peak of PDR concentrates at about 9.25 MeV. The explicit values of the centroid energy in each case will have a dependence on the energy region $[E_{\rm min}, E_{\rm max}]$ where the energy moment is measured, as well as the definition of "S part," i.e., the choice of the critical R, but the shift is very small (tens of keV) and does not change the main conclusion of the current investigation. It is well known that the theoretical evaluations of the integrated cross section $\int \sigma(\omega) d\omega$ are overestimated by about 20%–40% [8,43,49] compared to the classical one [47],

$$\sigma^{\rm int}_{\rm classical} \simeq 60 \frac{NZ}{A}\ ({\rm MeV\,mb}), \tag{16}$$

where N, Z, A are the neutron number, the proton number, and the mass number, respectively. Therefore, for convenience, the ratios of PDR integrated cross sections are compared with the energy weighted sum rule (EWSR) exhausted by PDR (the total value of EWSR exhausted by PDR and GDR is about 100%–105% in experimental measurements). In Table I, a comparison of PDR parameters between two distinct geometrical cases has been made. The calculated centroid energies are in good agreement with experimental measurements in both cases if one relates the experimental result of the γ decay to the prolate geometry and relates the result of the neutron decay to the spherical geometry. In the prolate case, the integrated cross section corresponding to PDR is about 4.90%, which stays at the same level as the EWSR exhausted by PDR that was measured in experiment, namely, 5.0(1.5)%. In the spherical case, the calculated result (6.77%) is larger than the experimental value [2.8(5)%] [16]. The discrepancy between different PDR energies in the same nucleus ^{68}Ni from different measurement methods implies that our understanding about the low-lying electric dipole excitation in the shape-coexistent nucleus ^{68}Ni should be improved. In this work, we approximate the excitation of the ^{68}Ni shape isomer by a one-particle–one-hole transition built on the prolate deformed isomeric state. The structure of PDR is separated from the whole spectrum according to the strong isoscalar character. The large deformation makes the dipole resonance structure split; the peak of PDR is pushed to a higher position compared to the spherical case. Our calculation may shed some light on the nature of the pygmy resonance built on the shape isomeric state.

TABLE I. The comparison of PDR parameters in two different geometry cases. The experimental data are extracted from [16] and [9,11].

	$E_{\rm cen}$ (MeV)	$\sigma^{\rm int}_{\rm PDR}$ (mb MeV)	$\sigma^{\rm int}_{\rm PDR}/\sigma^{\rm int}_{\rm Total}$ (%)	Expt. (MeV)	$S_{\rm EWSR}$ (%)
SPH.	9.25	84.8	6.77	9.55(17)	2.8(5)
PRO.	10.89	61.0	4.90	11.0(5)	5.0(1.5)

III. DISCUSSION

We notice that in the previously mentioned experiments the averaged kinematic energies of the ^{68}Ni ions before the virtual γ absorption happened are very close (600 MeV/u in the γ decay reaction [17] and 502.7 MeV in the neutron decay reaction [16]). Therefore, unless the branching ratio of each reaction channel is very energy sensitive, the peak of PDR is unlikely to shift as high as about 1.5 MeV. When the unstable nuclei ^{68}Ni are produced by bombarding ^{86}Kr onto a Be target, shape isomeric states are expected to emerge. Due to the sufficiently long half-life time, once produced, they will survive to be transmitted to the electromagnetic reaction target. It was reported in Ref. [26] that the fraction of the ^{68}Ni isomeric 0^+_2 state is less than 1%, where ^{68}Ni is produced by the fragmentation of a 140 MeV/u ^{82}Se beam on a ^{9}Be target. This incidence energy is far less than the ones we mentioned previously, namely, 900 MeV/u in the γ decay case [17] and 650 MeV/u in the neutron decay case [16]. Therefore, if the isomeric ratio is energy sensitive, the shape isomers are expected to share a larger percentage in the incoming ^{68}Ni beams in the (γ^*, γ) case, so there should be an enhancement of the shape isomer's influence on PDR as the ratio increases, namely, pushing the PDR peak higher.

The second possibility is that the fragmentation of ^{68}Ni in neutron decay channel is incompatible with the shape isomeric state. In the γ decay channel, the nucleus is not perturbed far from the equilibrium position, i.e., the shape coexistence states. The excitation of prolate shape ^{68}Ni ions

via photon scattering will be detected. However, in neutron decay channels, ^{68}Ni fragments into ^{67}Ni or ^{66}Ni, the nucleons will be rearranged, and then the delicate shape isomeric state is destroyed. Therefore, the influence of the shape isomeric state on pygmy dipole resonance does not manifests itself in the (γ^*, n) or $(\gamma^*, 2n)$ channels. To identify the collapse of the shape isomeric state in this scenario, it is required to detect the corresponding transition events. Fortunately, the isomers always decay in particular patterns; e.g., for the ^{68}Ni nucleus, the 0_2^+ state decays through internal pair production, emitting the signature 511-keV γ line [23–25].

A way to check whether the energy-dependent isomeric ratio or the collapse of the isomeric state matters is to set up the electromagnetic excitation of ^{68}Ni by the same means, i.e., the same incident energy and the same target. If the measurements in the photon scattering and the photoneutron channel coincide with each other, it will be proof of the energy sensitive isomeric ratio; otherwise, if the measurements still mismatch, it might be a strong hint of the collapse of the shape isomeric state in the photoneutron reaction.

ACKNOWLEDGMENTS

We wish to acknowledge support from Prof. Daomu Zhao. This work is partially supported by the National Science Foundation of China.

[1] T. Hartmann, M. Babilon, S. Kamerdzhiev, E. Litvinova, D. Savran, S. Volz, and A. Zilges, Phys. Rev. Lett. **93**, 192501 (2004).
[2] P. Adrich, A. Klimkiewicz, M. Fallot, K. Boretzky, T. Aumann, D. Cortina-Gil, U. Datta Pramanik, T. W. Elze, H. Emling, H. Geissel, M. Hellström, K. L. Jones, J. V. Kratz, R. Kulessa, Y. Leifels, C. Nociforo, R. Palit, H. Simon, G. Surówka, K. Sümmerer, and W. Waluś (LAND-FRS Collaboration), Phys. Rev. Lett. **95**, 132501 (2005).
[3] D. Savran, M. Babilon, A. M. van den Berg, M. N. Harakeh, J. Hasper, A. Matic, H. J. Wörtche, and A. Zilges, Phys. Rev. Lett. **97**, 172502 (2006).
[4] J. Gibelin, D. Beaumel, T. Motobayashi, Y. Blumenfeld, N. Aoi, H. Baba, Z. Elekes, S. Fortier, N. Frascaria, N. Fukuda, T. Gomi, K. Ishikawa, Y. Kondo, T. Kubo, V. Lima, T. Nakamura, A. Saito, Y. Satou, J.-A. Scarpaci, E. Takeshita, S. Takeuchi, T. Teranishi, Y. Togano, A. M. Vinodkumar, Y. Yanagisawa, and K. Yoshida, Phys. Rev. Lett. **101**, 212503 (2008).
[5] N. Paar, Y. F. Niu, D. Vretenar, and J. Meng, Phys. Rev. Lett. **103**, 032502 (2009).
[6] B. Löher, D. Savran, T. Aumann, J. Beller, M. Bhike, N. Cooper, V. Derya, M. Duchêne, J. Endres, A. Hennig, P. Humby, J. Isaak, J. Kelley, M. Knörzer, N. Pietralla, V. Ponomarev, C. Romig, M. Scheck, H. Scheit, J. Silva, A. Tonchev, W. Tornow, F. Wamers, H. Weller, V. Werner, and A. Zilges, Phys. Lett. B **756**, 72 (2016).
[7] A. Klimkiewicz, N. Paar, P. Adrich, M. Fallot, K. Boretzky, T. Aumann, D. Cortina-Gil, U. Datta Pramanik, T. W. Elze, H. Emling, H. Geissel, M. Hellström, K. L. Jones, J. V. Kratz, R. Kulessa, C. Nociforo, R. Palit, H. Simon, G. Surówka, K. Sümmerer, D. Vretenar, and W. Waluś (LAND Collaboration), Phys. Rev. C **76**, 051603 (2007).
[8] J. Piekarewicz, Phys. Rev. C **83**, 034319 (2011).
[9] O. Wieland and A. Bracco, Prog. Part. Nucl. Phys. **66**, 374 (2011), particle and Nuclear Astrophysics.
[10] V. Baran, M. Colonna, M. Di Toro, A. Croitoru, and D. Dumitru, Phys. Rev. C **88**, 044610 (2013).
[11] A. Carbone, G. Colò, A. Bracco, L.-G. Cao, P. F. Bortignon, F. Camera, and O. Wieland, Phys. Rev. C **81**, 041301 (2010).
[12] P. G. Hansen and B. Jonson, Europhys. Lett. **4**, 409 (1987).
[13] Y. Suzuki and Y. Tosaka, Nucl. Phys. A **517**, 599 (1990).
[14] J. Endres, D. Savran, A. M. ven den Berg, P. Dendooven, M. Fritzsche, M. N. Harakeh, J. Hasper, H. J. Wörtche, and A. Zilges, Phys. Rev. C **80**, 034302 (2009).
[15] E. G. Lanza, A. Vitturi, E. Litvinova, and D. Savran, Phys. Rev. C **89**, 041601 (2014).
[16] D. M. Rossi, P. Adrich, F. Aksouh, H. Alvarez-Pol, T. Aumann, J. Benlliure, M. Böhmer, K. Boretzky, E. Casarejos, M. Chartier, A. Chatillon, D. Cortina-Gil, U. Datta Pramanik, H. Emling, O. Ershova, B. Fernandez-Dominguez, H. Geissel, M. Gorska, M. Heil, H. T. Johansson, A. Junghans, A. Kelic-Heil, O. Kiselev, A. Klimkiewicz, J. V. Kratz, R. Krücken, N. Kurz, M. Labiche, T. Le Bleis, R. Lemmon, Y. A. Litvinov, K. Mahata, P. Maierbeck, A. Movsesyan, T. Nilsson, C. Nociforo, R. Palit, S. Paschalis, R. Plag, R. Reifarth, D. Savran, H. Scheit, H. Simon, K. Sümmerer, A. Wagner, W. Waluś, H. Weick, and M. Winkler, Phys. Rev. Lett. **111**, 242503 (2013).
[17] O. Wieland, A. Bracco, F. Camera, G. Benzoni, N. Blasi, S. Brambilla, F. C. L. Crespi, S. Leoni, B. Million, R. Nicolini, A. Maj, P. Bednarczyk, J. Grebosz, M. Kmiecik, W. Meczynski, J. Styczen, T. Aumann, A. Banu, T. Beck, F. Becker, L. Caceres, P. Doornenbal, H. Emling, J. Gerl, H. Geissel, M. Gorska, O. Kavatsyuk, M. Kavatsyuk, I. Kojouharov, N. Kurz, R. Lozeva, N. Saito, T. Saito, H. Schaffner, H. J. Wollersheim, J. Jolie, P. Reiter, N. Warr, G. deAngelis, A. Gadea, D. Napoli, S. Lenzi, S. Lunardi, D. Balabanski, G. LoBianco, C. Petrache, A. Saltarelli, M. Castoldi, A. Zucchiatti, J. Walker, and A. Bürger, Phys. Rev. Lett. **102**, 092502 (2009).
[18] T. Nikšić, N. Paar, D. Vretenar, and P. Ring, Comput. Phys. Commun. **185**, 1808 (2014).
[19] P. Walker and G. Dracoulis, Nature **399**, 35 (1999).
[20] G. D. Dracoulis, B. Fabricius, A. E. Stuchbery, A. O. Macchiavelli, W. Korten, F. Azaiez, E. Rubel, M. A. Deleplanque, R. M. Diamond, and F. S. Stephens, Phys. Rev. C **44**, 1246(R) (1991).
[21] K. Heyde, J. Jolie, R. Fossion, S. De Baerdemacker, and V. Hellemans, Phys. Rev. C **69**, 054304 (2004).
[22] I. O. Morales, A. Frank, C. E. Vargas, and P. Van Isacker, Phys. Rev. C **78**, 024303 (2008).
[23] R. Grzywacz, R. Béraud, C. Borcea, A. Emsallem, M. Glogowski, H. Grawe, D. Guillemaud-Mueller, M. Hjorth-Jensen, M. Houry, M. Lewitowicz, A. C. Mueller, A. Nowak, A. Płochocki, M. Pfützner, K. Rykaczewski, M. G. Saint-Laurent, J. E. Sauvestre, M. Schaefer, O. Sorlin, J. Szerypo, W. Trinder, S. Viteritti, and J. Winfield, Phys. Rev. Lett. **81**, 766 (1998).
[24] S. Suchyta, S. N. Liddick, Y. Tsunoda, T. Otsuka, M. B. Bennett, A. Chemey, M. Honma, N. Larson, C. J. Prokop, S. J. Quinn, N. Shimizu, A. Simon, A. Spyrou, V. Tripathi, Y. Utsuno, and J. M. VonMoss, Phys. Rev. C **89**, 021301 (2014).

[25] F. Recchia, C. J. Chiara, R. V. F. Janssens, D. Weisshaar, A. Gade, W. B. Walters, M. Albers, M. Alcorta, V. M. Bader, T. Baugher, D. Bazin, J. S. Berryman, P. F. Bertone, B. A. Brown, C. M. Campbell, M. P. Carpenter, J. Chen, H. L. Crawford, H. M. David, D. T. Doherty, C. R. Hoffman, F. G. Kondev, A. Korichi, C. Langer, N. Larson, T. Lauritsen, S. N. Liddick, E. Lunderberg, A. O. Macchiavelli, S. Noji, C. Prokop, A. M. Rogers, D. Seweryniak, S. R. Stroberg, S. Suchyta, S. Williams, K. Wimmer, and S. Zhu, Phys. Rev. C **88**, 041302 (2013).
[26] F. Recchia, D. Weisshaar, A. Gade, J. A. Tostevin, R. V. F. Janssens, M. Albers, V. M. Bader, T. Baugher, D. Bazin, J. S. Berryman, B. A. Brown, C. M. Campbell, M. P. Carpenter, J. Chen, C. J. Chiara, H. L. Crawford, C. R. Hoffman, F. G. Kondev, A. Korichi, C. Langer, T. Lauritsen, S. N. Liddick, E. Lunderberg, S. Noji, C. Prokop, S. R. Stroberg, S. Suchyta, K. Wimmer, and S. Zhu, Phys. Rev. C **94**, 054324 (2016).
[27] G. A. Lalazissis, T. Nikšić, D. Vretenar, and P. Ring, Phys. Rev. C **71**, 024312 (2005).
[28] G. A. Lalazissis, J. König, and P. Ring, Phys. Rev. C **55**, 540 (1997).
[29] D. L. Hill and J. A. Wheeler, Phys. Rev. **89**, 1102 (1953).
[30] P. Ring and P. Schuck, *The Nuclear Many-Body Problem* (Springer, Berlin, 2004).
[31] C. D. Conti, A. Galeão, and F. Krmpotić, Phys. Lett. B **444**, 14 (1998).
[32] H. Liang, N. Van Giai, and J. Meng, Phys. Rev. Lett. **101**, 122502 (2008).
[33] N. Paar, P. Ring, T. Nikšić, and D. Vretenar, Phys. Rev. C **67**, 034312 (2003).
[34] N. Paar, T. Nikšić, D. Vretenar, and P. Ring, Phys. Rev. C **69**, 054303 (2004).
[35] Z. M. Niu, Y. F. Niu, H. Z. Liang, W. H. Long, and J. Meng, Phys. Rev. C **95**, 044301 (2017).
[36] K. Yoshida and N. V. Giai, Phys. Rev. C **78**, 064316 (2008).
[37] K. Yoshida and T. Nakatsukasa, Phys. Rev. C **83**, 021304 (2011).
[38] T. Nakatsukasa, T. Inakura, and K. Yabana, Phys. Rev. C **76**, 024318 (2007).
[39] X. Sun and D. Lu, Phys. Rev. C **96**, 024614 (2017).
[40] H. Sagawa, N. Van Giai, N. Takigawa, M. Ishihara, and K. Yazaki, Z. Phys. A **351**, 385 (1995).
[41] S. Ebata, T. Nakatsukasa, T. Inakura, K. Yoshida, Y. Hashimoto, and K. Yabana, Phys. Rev. C **82**, 034306 (2010).
[42] J. Piekarewicz, Phys. Rev. C **73**, 044325 (2006).
[43] T. Inakura, T. Nakatsukasa, and K. Yabana, Phys. Rev. C **84**, 021302 (2011).
[44] J. Boguta and A. Bodmer, Nucl. Phys. A **292**, 413 (1977).
[45] D. Pena Arteaga and P. Ring, Phys. Rev. C **77**, 034317 (2008).
[46] S. Xuwei, C. Jing, and L. Dinghui, Chin. Phys. C **42**, 014101 (2018).
[47] B. R. Mottelson and A. N. Bohr, *Nuclear Structure* (World Scientific, Singapore, 1998).
[48] D. Vretenar, A. Afanasjev, G. Lalazissis, and P. Ring, Phys. Rep. **409**, 101 (2005).
[49] M. N. Harakeh and A. van der Woude, *Giant Resonances: Fundamental High-Frequency Modes of Nuclear Excitation* (Oxford University Press, Oxford, 2001).